

Strain-induced low-frequency relaxation in colloidal DGEBA/SiO₂ suspensions

Rick Dannert · Roland Sanctuary ·
Matthieu Thomassey · Patrick Elens ·
Jan Kristian Krüger · Jörg Baller

Received: 6 March 2014 / Revised: 5 May 2014 / Accepted: 2 July 2014 / Published online: 1 August 2014
© Springer-Verlag Berlin Heidelberg 2014

Abstract Diglycidyl ether of bisphenol A (DGEBA) is widely exploited as an epoxy resin in adhesives and coatings. In this paper, it is used as an oligomer matrix for silica-filled nanocomposites. Rheological measurements show that the pure matrix obeys power-law relaxation dynamics in the vicinity of the dynamic glass transition of this low-molecular-weight glass former. In the filled systems, a low-frequency relaxation appears additionally to the structural α -process of the matrix. Considering the nanocomposites as Newtonian hard-sphere suspensions at low angular frequencies (or high temperatures), the modified terminal regime behavior of the matrix can be linked to strain-induced perturbations of the isotropic filler distributions. While in the low-frequency regime hydrodynamic stresses relax instantaneously, the Brownian stress relaxation is viscoelastic and can be evidenced by dynamic rheological measurements. At higher angular frequencies, the α -process of the matrix

superimposes on the Brownian stress relaxation. In particular, we were able to depict the low-frequency anomaly for concentrated, semi-dilute, and even for dilute suspensions.

Keywords Rheology · Brownian motion · Colloidal suspension · Nanoparticles · Low-molecular-weight glass former · Relaxation process

Introduction

Nanocomposites become increasingly important for technical applications. Regarding their physical properties, most interest is focused on the mechanical performances (e.g., Wetzel et al. 2003; Kinloch et al. 2006, 2008; Johnsen et al. 2007; Dudkin et al. 2008). A systematic improvement of their mechanical properties requires a deeper understanding of the elastic, viscoelastic, and flow behaviors of the nanocomposites. Beside the technological aspects of these behaviors, there exists a fundamental interest in the relationship between the mechanical properties of the nanocomposites, the matrix/filler (Suzuki et al. 2005), or filler/filler interactions (Chabert et al. 2004) and the associated structure modifications (e.g., network formation (Jaber et al. 2011) and interphase formation (Alberola et al. 2001)). The investigation of the influence nanoparticles takes on the thermally or dynamically induced transition from liquid into viscoelastic into solid state represents a useful approach to shed light on the mentioned structure-property relationship.

In the present paper, we have chosen rheology as an experimental tool to determine the dynamic shear stiffness evolution as a function of temperature between the liquid and glassy states. As a hybrid model system, we have selected an oligomer-based nanocomposite, the epoxy

R. Dannert · R. Sanctuary · M. Thomassey · P. Elens ·
J. K. Krüger · J. Baller (✉)
Physics and Materials Science Research Unit,
Laboratory for the Physics of Advanced Materials, University of
Luxembourg 162A avenue de la Faïencerie, 1511 Luxembourg,
Grand-Duchy of Luxembourg
e-mail: joerg.baller@uni.lu

Present Address:
M. Thomassey
G2IP / ICPEES – CNRS UMR 7515 – ECPM, University of Strasbourg
25 rue Becquerel, 67087 Strasbourg Cedex 2, France

Present Address:
J. K. Krüger
Lehrstuhl Adhäsion und Interphasen in Polymeren,
Universität des Saarlandes, 66123 Saarbrücken, Deutschland

resin diglycidyl ether of bisphenol A (DGEBA) filled with silanized inorganic silica nanoparticles with an average diameter of about 25 nm. The matrix system DGEBA with a molecular weight of about 340 g/mol undergoes a glass transition at $T_g \approx 257$ K (Sanctuary et al. 2006), thus well below ambient temperature; the SiO_2 nanoparticles are solid and amorphous with glass transitions far above those of the pure and filled matrix material. Consequently, the nanoparticles' properties can be considered as independent of temperature in this study. Calorimetric investigations (Sanctuary et al. 2006; Baller et al. 2009, 2011) have been realized on DGEBA- SiO_2 composites up to a nanoparticle concentration of 40 wt %; almost no influence of the fillers on the glass transition of the DGEBA matrix has been found. Dynamic shear experiments (Schröter and Donth 2002) reveal a rather simple relaxation behavior of the matrix: increasing the shear angular frequency at constant temperature yields a direct transition from the terminal regime to the dynamically frozen state. For DGEBA filled with organically modified montmorillonites, physical gelation is observed instead of terminal behavior when the nanocomposites undergo isothermal frequency sweeps (Le Pluart et al. 2004).

The presence of the silica nanoparticles is expected to increase the dynamic viscosity of the liquid nanocomposite at low angular frequencies. Hence, the interesting question arises: how in the filled systems the complex shear modulus evolves as a function of temperature and angular frequency when, irrespective of the filler content, the glass transition temperature remains practically unaffected? In this context, it has to be stressed that at high temperatures, the DGEBA- SiO_2 nanocomposites can tentatively be considered as colloidal suspensions with particle distributions corresponding to maximum entropy in the unperturbed state. According to the filler content (extending from 0 to 40 wt %), the samples studied in this paper are dilute, semi-dilute, and concentrated suspensions. Strain-induced disturbances of the homogeneous particle distributions are expected to generate the Brownian stress. The Brownian stress relaxation has already been observed in concentrated spherical silica suspensions (Watanabe et al. 1996; Shikata and Pearson 1994). The main purpose of the present paper is to elucidate whether the Brownian stress relaxation takes influence on the rheological behavior of the DGEBA- SiO_2 composites and, if so, how it competes with the underlying α -process of the DGEBA matrix.

In the following, we will first show that the DGEBA matrix fairly obeys power-law relaxation dynamics when approaching the glass transition. Then we will describe the influence of the concentration of the silanized SiO_2 nanoparticles on the viscoelastic behavior of the nanocomposites. Finally, we will discuss the results in terms of a competition between the Brownian stress relaxation

resulting from strain-induced perturbation of the filler distribution and the matrix specific α -process.

Experimental

Material characterization

The nanocomposites discussed in this paper are based on a master batch of a distilled type of DGEBA filled with 40 wt % of silica nanoparticles (Nanopox A410, Nanoresins AG, Geesthacht, Germany). According to the manufacturer, this corresponds to 25 vol % of fillers. The silica is quasi-spherical particles with an average diameter of about 25 nm including a hydrophobic silane layer (Baller et al. 2009, 2011). From Fig. 1, it becomes clear that their size distribution is rather narrow and they are homogeneously distributed inside the DGEBA matrix (Baller et al. 2009, 2011). The nanoparticles are created within the DGEBA matrix by means of a sol-gel process (Sprenger et al. 2003; Hanse 2002). The particle aggregation inside the matrix is prevented by the latter creation process and the silane layers at the surfaces of the fillers (Baller et al. 2009).

DGEBA- x % SiO_2 systems ($x = 100 \cdot m_{\text{SiO}_2} / (m_{\text{SiO}_2} + m_{\text{DGEBA}}) = 5, 10, 20, 30$) are obtained by adequately diluting the master batch with the same distilled DGEBA as used for the master batch. To homogenize the suspensions, a planetary mixer (SpeedMixer, Hauschild, Germany) is exploited. After perfectly mixing the samples, they are degassed during half an hour at 354 K. This temperature was also chosen to remelt possibly existing DGEBA crystallites ($T_{\text{melt}} = 317$ K). Under usual cooling conditions, recrystallization is avoided (Baller et al. 2011). Thus, at temperatures higher than T_g , the nanocomposites consist of nanoparticles of SiO_2 surrounded by a liquid DGEBA matrix.

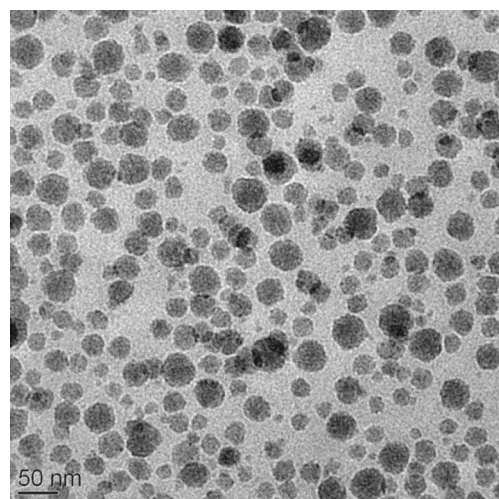


Fig. 1 TEM picture of a DGEBA-40 wt % SiO_2 sample

Rheology

Dynamic rheological experiments are performed with an Anton Paar MCR 302 rheometer using parallel plate geometries. Depending on the dynamic stiffness of the samples, 8-, 25-, or 50-mm diameter plates are chosen. When introducing the samples between the plates at ambient temperature, a gap width of 1 mm is respected. The measurements are carried out in a temperature-controlled test chamber pervaded with dry N₂ gas. The angular frequency window of the instrument exploited for the measurements extends from $\omega = 0.314$ rad/s to $\omega = 62.8$ rad/s (50 mHz to 10 Hz). Isothermal angular frequency sweeps are carried out at different temperatures T in order to determine the complex shear modulus $G^*(\omega) = G'(\omega) + iG''(\omega)$, where $G'(\omega)$ and $G''(\omega)$ represent the storage and the loss shear modulus, respectively. Generally, the measurements are carried out in the constant strain mode. The amplitude γ_0 of the sinusoidal strain $\gamma(t) = \gamma_0 \sin \omega t$ is always chosen to strictly respect the linear response regime for each angular frequency ω and at any given temperature T . Under this condition, the stress response is given by $\sigma(t) = \sigma_0 \sin(\omega t + \delta)$, δ representing the phase angle shift with respect to strain.

Results

Figure 2a and b represent double-logarithmic plots of G' and G'' as a function of angular frequency for pure DGEBA and the DGEBA-30 % SiO₂ samples, respectively. The curves have been obtained from isothermal angular frequency sweeps at temperatures ranging from 259 to 273 K for pure DGEBA and from 259 to 303 K for DGEBA-30 % SiO₂.

Figure 3 shows the master curves $G'(a_T\omega)$ and $G''(a_T\omega)$ for the matrix at a reference temperature $T_0 = 273$ K. To construct the master curves, we have exploited the temperature-frequency equivalence principle which allows superposing the storage and loss shear data by horizontal shifts $\log a_T$ along the angular frequency axis. Vertical shifts of the data were not necessary. The same procedure was applied to collapse the shear data of the DGEBA-30 % SiO₂ sample into master curves which are depicted in Fig. 4 together with the storage and loss moduli of the other nanocomposites under investigation ($x = 5, 10, 20, 40$).

In Fig. 3, the evolution of the normalized phase angle $2\delta/\pi$ as a function of angular frequency is indicative for a glass transition (α -process). At low angular frequencies, DGEBA behaves as a liquid ($2\delta/\pi \approx 1$). At high angular frequencies, the oligomer resin dynamically freezes and behaves as a solid ($2\delta/\pi \approx 0$). Several molecular glass formers have been shown to obey power-law relaxation dynamics when approaching the glass transition (Winter

2013). In Fig. 3, the solid lines represent a fit for the storage and loss moduli of the low-molecular-weight glass former DGEBA using

$$G'(\omega) = \int_0^\infty \frac{H(\tau)}{\tau} \cdot \frac{(\omega\tau)^2}{1+(\omega\tau)^2} \cdot d\tau$$

$$G''(\omega) = \int_0^\infty \frac{H(\tau)}{\tau} \cdot \frac{\omega\tau}{1+(\omega\tau)^2} \cdot d\tau$$
(1)

and the broadened power-law spectrum

$$H(\tau) = H_0 \left(\frac{\tau}{\tau_{\max}} \right)^n e^{-\left(\frac{\tau}{\tau_{\max}}\right)^\beta}$$
(2)

For the reference temperature $T_0 = 273$ K, the parameters $H_0 = 5.5 \cdot 10^8$ Pa; $n = 0.51$; $\tau_{\max} = 7.3 \cdot 10^{-5}$ s; and $\beta = 0.68$ yield the best fit to the experimental data points. At least in the immediate vicinity of the dynamic glass transition, the shear modulus data are fairly described by the power-law spectrum (2).

At very low frequencies, terminal regime scaling is expected for the low-molecular-weight glass former DGEBA. From Eq. 1, it follows that

$$G'(\omega) = \omega^2 \int_0^\infty H_0 \left(\frac{\tau}{\tau_{\max}} \right)^n \left(e^{-\frac{\tau}{\tau_{\max}}} \right)^\beta \tau d\tau \propto \omega^2$$

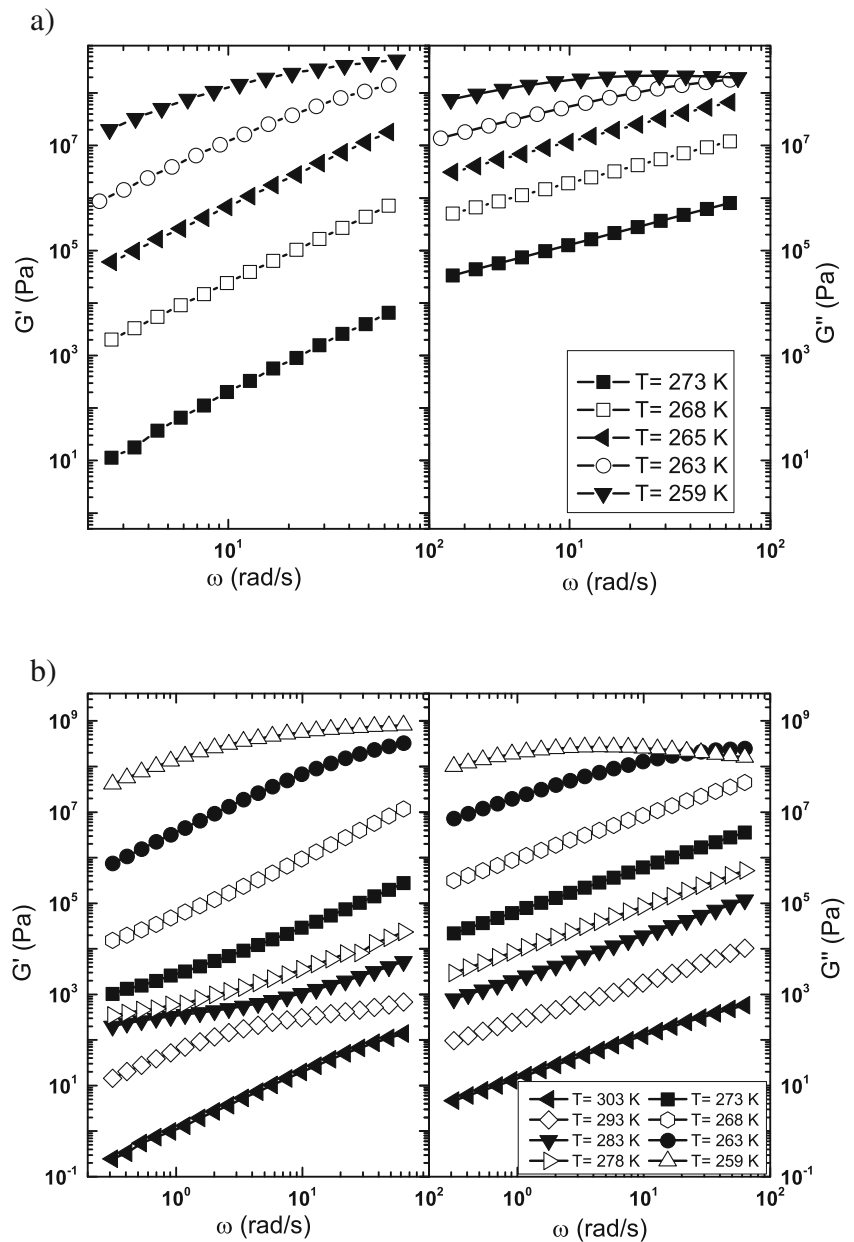
$$G''(\omega) = \omega \int_0^\infty H_0 \left(\frac{\tau}{\tau_{\max}} \right)^n \left(e^{-\frac{\tau}{\tau_{\max}}} \right)^\beta d\tau \propto \omega$$
(3)

The results presented in Fig. 3 yield $G' \propto \omega^{1.8}$ and $G'' \propto \omega^{1.0}$ (in agreement with those of Schröter and Donth 2002).

The most prominent feature revealed by the dynamic data of the filled systems in Fig. 4 is the occurrence of an intermediate plateau-like elastic behavior which, irrespective of the nanoparticle content, emerges from a low-frequency regime tail $G' \propto \omega^{1.3}$ ($\omega \rightarrow 0$). The higher the nanoparticle concentration, the higher the “plateau” values are. Moreover, the onset angular frequency of the process (which tentatively can be defined as the angular frequency at which $G'(a_T\omega)$ starts deviating from the linear low-frequency regime tail) is slightly shifted towards “lower” frequencies upon increasing the filler content.

When increasing the angular frequency, $G'(a_T\omega)$ curves of the various filled systems start to converge and can, at least in the immediate proximity of the dynamic glass transition and for not too high nanoparticle concentrations, fairly be described by the relaxation dynamics of the matrix. The observation that the silica almost has no influence on the dynamical freezing of the matrix is in line with calorimetric data collected on DGEBA-SiO₂ composites up to a nanoparticle concentration of 30 % (Sanctuary et al. 2006; Baller et al. 2009, 2011). To interpret the invariance of the glass transition temperature, the authors claim that there is only such a small interaction between the SiO₂ nanoparticles and the DGEBA matrix that the glass transition of the nanocomposites is completely dominated by the α -process

Fig. 2 Real part G' and imaginary part G'' of the complex shear modulus of **a** pure DGEBA and **b** DGEBA-30 % SiO₂ as a function of angular frequency at different temperatures T



of the matrix. In case of the DGEBA-40 % SiO₂ system, calorimetric investigations show a slight shift of the glass transition towards a higher temperature (compared to the pure system). This behavior is confirmed by the rheological data in Fig. 4 with the restriction that the glass transition shift appears to be more pronounced than in the case of calorimetric measurements. The explanation of this feature claims for further investigation.

With increasing nanoparticle concentration, reinforcement can be observed in both the storage and loss modulus. The reinforcement of G' extends over several orders of magnitude at very low angular frequencies and progressively decreases at higher frequencies. Composite models such as the Palierne model (Palierne 1989; Vignaux-Nassiet et al.

1998) predict a change of G' and G'' by the same factor. This is obviously not the case for our data. Therefore, the reinforcement could not be described by these models. In general, nanoparticles can have a confining effect on the matrix molecules. Confinement can slow down the molecular dynamics of the matrix leading to an increased glass transition temperature. Additionally, stress relaxation can be influenced by confinement resulting in increased shear moduli. Due to the small sizes of the DGEBA molecules, confinement is not expected to be responsible for the changed moduli in our case, at least for the lower filler concentrations. This conclusion is supported by the fact that the glass transition temperature is almost independent of the filler concentration. It has also to be stressed that for the

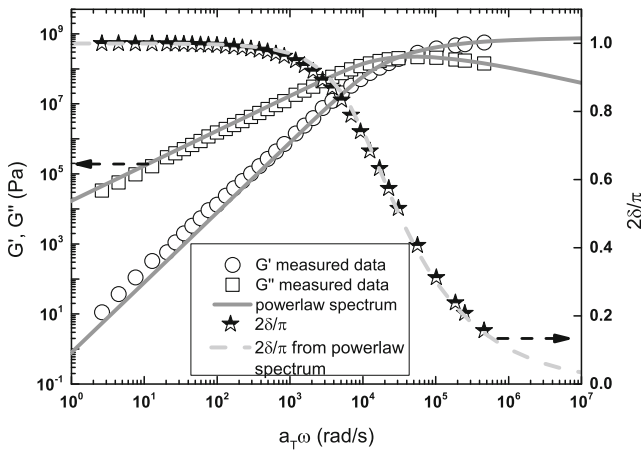


Fig. 3 Master curves $G'(a_T\omega)$, $G''(a_T\omega)$, and $2\delta(a_T\omega)/\pi$ (normalized phase angle) for pure DGEBA at a reference temperature $T_0 = 273$ K. The solid lines represent the storage and loss moduli data calculated from Eq. 1 and using the power-law spectrum (see Eq. 2) with parameters $H_0 = 5.5 \cdot 10^8$ Pa; $n = 0.51$; $\tau_{max} = 7.3 \cdot 10^{-5}$ s; and $\beta = 0.68$. The dashed line describes $2\delta(a_T\omega)/\pi$ data obtained from calculated $G'(a_T\omega)$ and $G''(a_T\omega)$ values

systems under study, analysis of the reinforcement effect is complicated due to the presence of the low-frequency anomaly. It is furthermore difficult to unambiguously determine the regime where this anomaly is effective.

We tend to interpret the low-frequency anomaly as an additional relaxation process which is strongly linked to the presence of the nanoparticles in the DGEBA matrix. According to the Kramers-Kronig relations, one would expect that a relaxation process visible in the real part of the complex shear modulus is also visible in its imaginary part. In the terminal regime, the real parts of the dynamic com-

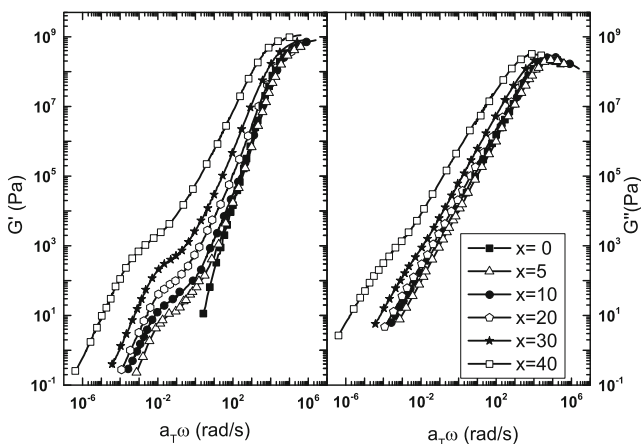


Fig. 4 Master curves $G'(a_T\omega)$ (left) and $G''(a_T\omega)$ (right) for DGEBA- x % of silica nanoparticles at the reference temperature $T_0 = 273$ K. The lines linking the measured points are guidelines for the eyes

plex viscosities can be obtained from the imaginary part of the shear modulus using

$$\eta' = \left(\frac{G''(a_T\omega)}{a_T\omega} \right) \tag{4}$$

From Fig. 5, it becomes clear that in case of the 30 % sample, G'' follows a transition from a regime with higher viscosity $\eta'_0 = \left(\frac{G''(a_T\omega)}{a_T\omega} \right)_{\omega \rightarrow 0}$ to a regime with lower viscosity $\eta'_{inf} = \left(\frac{G''(a_T\omega)}{a_T\omega} \right)_{\omega \rightarrow \infty}$ (restricted to terminal behavior). The transition regime corresponds to where the storage modulus G' levels off (see Fig. 5). The loss moduli of the 20 and 40 % samples show the same behavior (see Fig. 4). We assume that for the other samples ($x = 5, 10$), the changes of G'' induced by the low-frequency relaxation are too small to be experimentally resolved.

Deviations of the storage moduli from ideal terminal behavior (fractional power-law relationships $G' \propto \omega^{1.8}$ for the neat DGEBA matrix and $G' \propto \omega^{1.3}$ for each of the filled systems) reflect a limitation in the frequencies examined. The real low ω asymptote (that could emerge at low frequencies out of the examined range) would be $G' \propto \omega^2$ according to Eq. 3.

We assume that the low-frequency process is a filler-induced phenomenon rather than an intrinsic matrix effect enhanced by the nanoparticles. The need for this hypothesis ensues from the fact that due to experimental limits related to the very low stiffness of the pure system at high temperatures, storage modulus data are not available for DGEBA in the frequency range where the low-frequency process appears (see Fig. 4). However, to our best knowledge, there

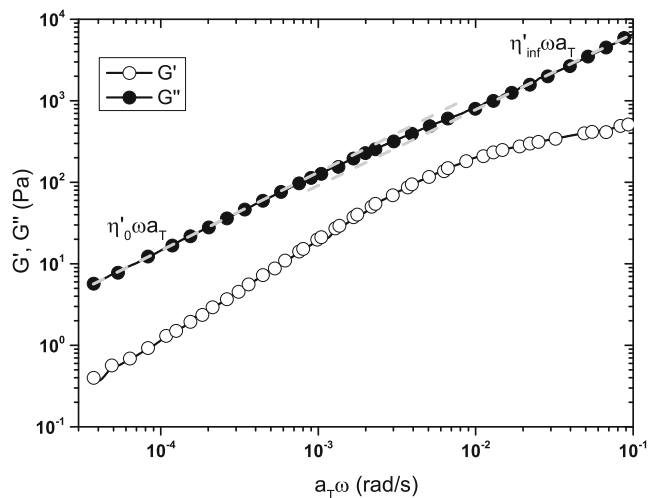


Fig. 5 Low-frequency parts of the master curves $G'(a_T\omega)$ and $G''(a_T\omega)$ obtained for the DGEBA-30 % SiO₂ sample at the reference temperature $T_0 = 273$ K. The gray dashed lines are drawn to highlight the transition from a higher (η'_0) to a lower viscosity (η'_{inf}) behavior when the angular frequency is increased within the terminal regime

is no reference in the literature to the existence of a low-frequency relaxation in low-molecular-weight DGEBA.

To further corroborate the assumption that the low-frequency process represents a relaxation phenomenon, we follow Shikata and Pearson (1994) and introduce a reduced loss modulus for the three samples with the highest concentration ($x = 20 - 40$) as follows:

$$\Delta G'' = G'' - \eta'_{\text{inf}} \omega, \quad (5)$$

where the subtracted term $\eta'_{\text{inf}} \omega$ describes the “high-frequency” behavior of the loss modulus G'' (in the terminal regime). The high-frequency viscosities η'_{inf} used to calculate $\Delta G''$ according to Eq. 4 are given in Table 2.

Figure 6 shows the evolution of the low-frequency moduli G' and $\Delta G''$ as a function of $a_T \omega$. The dashed lines in Fig. 6 link the intersection points $G'(a_T \omega) = \Delta G''(a_T \omega)$ to angular frequencies ω_{lf} which are tentatively considered to be characteristic for the low-frequency relaxation process.

From Fig. 6, it becomes clear that at low angular frequencies $a_T \omega < a_T \omega_{\text{lf}}$, the respective evolutions of G' and $\Delta G''$ qualitatively suggest classical relaxation behavior (compare, e.g., to Fig. 3). At higher angular frequencies, the “classical” relaxation behavior is disturbed. In Table 1, we have listed the relaxation angular frequencies ω_{lf} and relaxation times τ_{lf} .

After evidencing the occurrence of two distinct relaxation processes in DGEBA- x % SiO₂ nanocomposites, the question arises why we succeeded in representing the storage and loss shear moduli in single master curves. Inspection of Fig. 4 yields that both processes (with different characteristics) are widely separated on the angular frequency scale. As a matter of fact, they cannot be seen simultaneously in a single isothermal angular frequency scan (see Fig. 2b). This nonoverlapping of the α - and low-frequency

Table 1 Low-frequency process: the relaxation angular frequencies ω_{lf} and relaxation times τ_{lf} for the three samples with the highest concentrations ($x = 20, 30, 40$) tentatively obtained from the intersection points $G'(a_T \omega) = \Delta G''(a_T \omega)$ in Fig. 6

x (-)	lf (1/s)	τ_{lf} (s)
20	0.0219	45.5
30	0.0103	97.6
40	0.0017	868

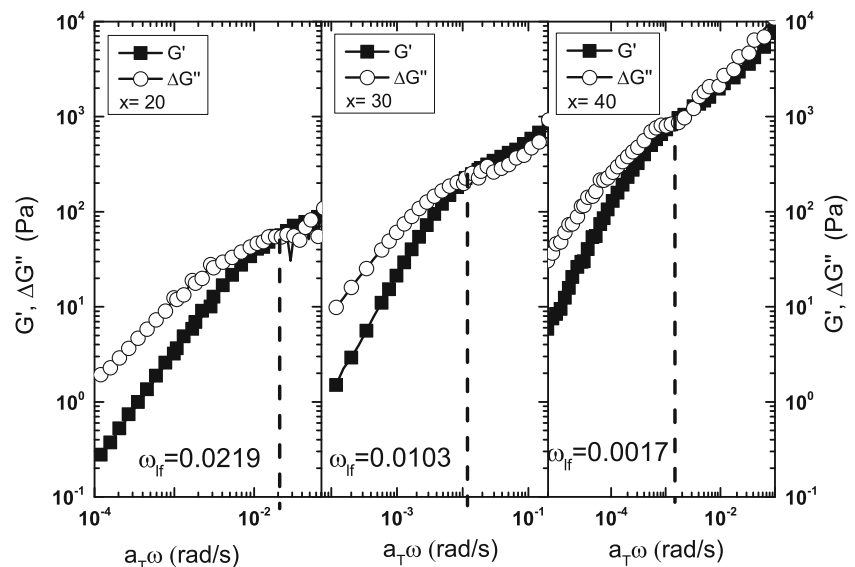
processes implicates that an unambiguous master curve can always be created, even if this does not make sense scientifically. This holds even true if the temperature dependences of the two processes are completely different (Ngai and Plazek 1995). Such a situation could, however, be seen in the temperature dependence of the horizontal shift parameters a_T as a discontinuity between the low temperature and high temperature regimes.

In Fig. 7, we have represented the horizontal shift factors a_T as a function of temperature for the various systems. Irrespective of the nanoparticle concentration, the $\log a_T(T)$ curves superimpose fairly well. There is no discontinuity visible. From the literature (Corezzi et al. 2002), it is known that the low-molecular-weight glass former DGEBA verifies the Vogel-Fulcher-Tammann law. It follows that the corresponding horizontal shift factors obey the Williams-Landel-Ferry (WLF) equation. Due to the fact that all curves in Fig. 7 coincide, the WLF behavior is respected by all nanocomposites under study.

$$\log a_T = -C_1 \frac{T - T_0}{T - T_0 + C_2} \quad (6)$$

In Fig. 7, the continuous line corresponds to a WLF plot with parameters $C_1 = 8.63$ and $C_2 = 44.08$ K. The

Fig. 6 Low-frequency data $G'(a_T \omega)$ and $\Delta G''(a_T \omega)$ for DGEBA- x % of SiO₂ samples ($x = 20, 30, 40$) at the reference temperature $T_0 = 273$ K. The dashed lines link the intersection points $G'(a_T \omega) = \Delta G''(a_T \omega)$ to angular frequencies ω_{lf} which are tentatively considered to be characteristic for the low-frequency relaxation process



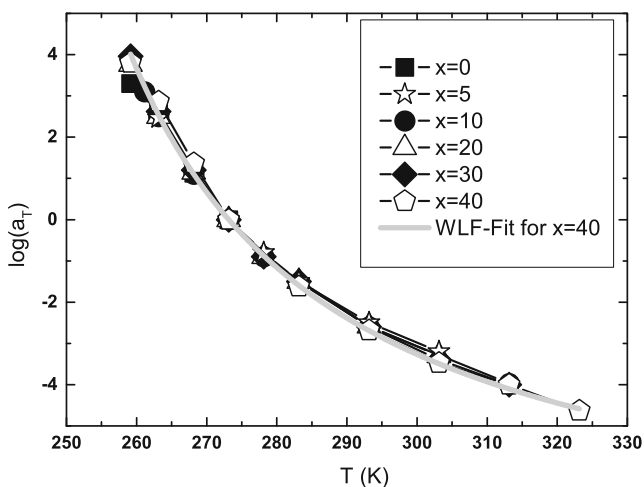


Fig. 7 Horizontal shift factors a_T used for the construction of the master curves (Fig. 4) of $G'(a_T\omega)$ and $G''(a_T\omega)$ for DGEBA- x % of silica nanoparticles at the reference temperature $T_0 = 273$ K. The gray line represents a WLF plot for $x = 40$ with parameters $C_1 = 8.63$ and $C_2 = 44.08$ K

coincidence of the shift factors for the matrix and the suspensions implies that the low-frequency relaxation has the same temperature dependence as the α -process. Obviously, the temperature dependence of the low-frequency relaxation has its origin in the temperature dependence of the matrix's viscosity (see Eq. 7).

Discussion

In the literature, one can find numerous references (Inoubli et al. 2006; Shikata and Pearson 1994; van der Werff et al. 1989; Graebbling et al. 1993; Watanabe et al. 1996; Vignaux-Nassiet et al. 1998) on suspensions showing secondary relaxation processes which are similar to the one described in this paper. Watanabe et al. (1997) discuss the frequency dependence of the storage and loss moduli G' and G'' of spherical styrene-isoprene micelles randomly dispersed in a nonentangling homopolyisoprene matrix. The dispersion exhibits two relaxation mechanisms that are attributed to the micelles with glassy styrene cores and soft isoprene corona. While the fast process corresponds to the relaxation of individual corona blocks, the slow one is attributed to the relaxation of anisotropy of the distribution of micelles.

Deformation relaxation (i) and decay of the Brownian stress (ii) indeed represent key mechanisms contributing to explain the physical background of strain-induced relaxations in suspensions. Each of both effects has individually been found in silica suspensions.

- (i) Vignaux-Nassiet et al. (1998) observed on polybutadiene melts filled with micro-sized spherical silica similar rheological behavior as we have described here for

the oligomer matrix DGEBA filled with nano-sized silica. Using appropriated models, the authors justify that the additional low-frequency relaxation domain is linked to the deformation relaxation of a thin layer of polymer chains weakly interacting with the silica surfaces via the Van der Waals dispersion forces. Due to the large size of the silica particles, the Brownian diffusion effects could be neglected.

- (ii) The investigation of linear viscoelastic behavior of concentrated submicron silica suspensions in super-cooled ethylene glycol/glycerol mixtures (Shikata and Pearson 1994, Watanabe et al. 1996, 1997) revealed the existence of a low-frequency relaxation process. The authors describe the colloids as viscoelastic suspensions of hard-sphere like Brownian particles with no long-range interaction (except the hydrodynamic interaction) and attribute the process to the relaxation of the shear-induced anisotropy in the distribution of particle positions. It has to be stressed that in the temperature range where the investigation took place, the low-frequency relaxation was obviously not in competition with the α -process of the ethylene glycol/glycerol mixture.

In contrast to the systems treated in the literature above, the DGEBA- x % SiO_2 systems comprise a matrix representing a low-molecular-weight glass former and nano-sized fillers (average radius $\bar{a} = 12.5$ nm) with ultrathin silane layers (thickness 0.6–2 nm (private communication of Dr. Sprenger from Evonik Hanse GmbH, Germany)) at their surfaces.

The thickness of the silane layer at the surface of the silica nanoparticles being extremely small, we tend to exclude strain-induced low-frequency form relaxation. A dynamical freezing of a hypothetical interphase emerging between the nanoparticles and the DGEBA matrix is expected to be observed by other experimental probes working in the same frequency regime as the shear rheology experiments presented in this work. However, temperature-modulated differential scanning calorimetry (TMDSC) (Sanctuary et al. 2006; Baller et al. 2009) as well as temperature modulated refractometry (Müller et al. 2013)—both operating in the frequency interval of interest and sensitive to the glass transition process—failed to provide evidence for the low-frequency relaxation phenomenon described in this paper.

In order to confirm the decay of the Brownian stress as origin of the low-frequency relaxation process, Shikata and Pearson (1994) evaluated the Peclet relaxation times:

$$\tau_p \approx \frac{\pi \eta'_{\text{inf}} a^3}{k_B T}, \quad (7)$$

where a represents the radius of a spherical particle.

Assuming that at low angular frequencies (or high temperatures) the filled samples described in this paper behave as model hard-sphere suspensions, we can again follow Shikata and Pearson (1994) and tentatively evaluate the Pecelet relaxation times (according to Eq. 7) and angular frequencies $\omega_p = \tau_p^{-1}$ as a function of the filler concentration. The results are presented in Table 2.

Interestingly the calculated values ω_p fairly correspond to the angular frequencies at which the storage shear moduli start to level off (see Fig. 8). Moreover, for the three nanocomposites with the highest filler concentration, the angular relaxation frequencies obtained from the experimental data shown in Fig. 6 and listed in Table 1 are in good agreement with the calculated Pecelet angular relaxation frequencies. This observation is in favor of the interpretation that in case of the nanocomposites, the low-frequency anomaly corresponds to viscoelastic relaxation of the Brownian stress resulting from strain-induced disturbance of the isotropic distribution of the nanoparticles. At angular frequencies $\omega > \omega_p$, the free energy stored in the systems as a result of the distorted configuration of the nanoparticles (Van der Werff et al. 1989) can no longer relax.

The deviation of the storage moduli $G'(a_T\omega)$ from ideal plateau-like behavior (see Figs. 6 and 8) can be due on one side to the distribution of the sizes of the nanoparticles (Lionberger and Russel 1997) and on the other side to the increasing influence of the viscoelastic behavior of the matrix upon rising the angular frequency (or decreasing the temperature). It can be observed that the values of the storage moduli at the Pecelet angular frequencies (see Fig. 8) increase with increasing nanoparticle content. Since we cannot deconvolute the α -process and the low-frequency process, we avoid to identify the plateau values of the storage moduli with the G'_∞ of the low-frequency relaxator (Lionberger and Russel 1997). Further increasing the angular frequency yields a complete domination of the α -process: the $G'(a_T\omega)$ and $G''(a_T\omega)$ master curves of the

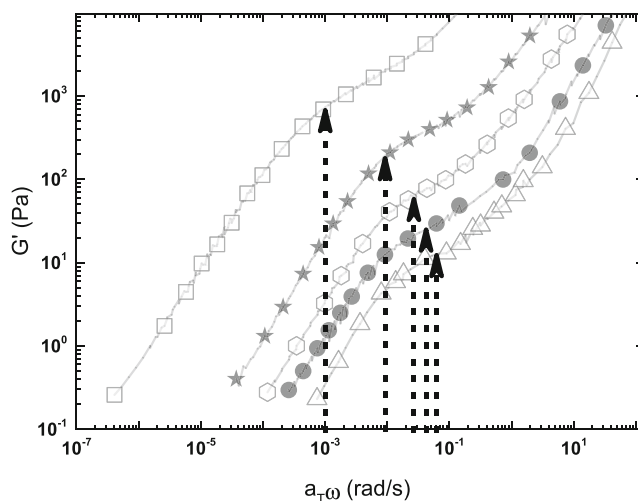


Fig. 8 Low-frequency $G'(a_T\omega)$ data (see also Fig. 4) for the various DGEBA- x % SiO₂ samples at the reference temperature $T_0 = 273$ K. The dashed arrows indicate the Pecelet angular frequencies for each concentration (see Table 2)

nanocomposites start to merge with the respective ones of the pure matrix.

Conclusion

Temperature/frequency behavior of the complex shear moduli of DGEBA- x % SiO₂ nanocomposites has been investigated by rheology. Master curves could be constructed to depict the linear viscoelastic response of the samples in an angular frequency interval exceeding the rheometer's frequency window by many decades. Up to a filler concentration of 30 %, the nanocomposites obey the same power-law relaxation dynamics (α -process) as the DGEBA matrix near the dynamic glass transition. Only the sample with the highest nanoparticle content ($x = 40$) deviates from the dynamic glass transition behavior of neat DGEBA. Thus, the insensitivity of the dynamical glass transition on the SiO₂ nanoparticle concentration predicted by calorimetric measurements (in case of $x \leq 30$) could be confirmed by the rheological investigations of the dynamical shear stiffness. Most interestingly, at low shear angular frequencies, the filled systems show a plateau-like elastic behavior which, for each sample, emerges from a “terminal” regime tail ($G' \propto \omega^{1.3}$). The phenomenon is interpreted as a low-frequency relaxation process. Considering the filled systems as model hard-sphere Newtonian suspensions at high temperatures (or low frequencies), we were able to evaluate Pecelet relaxation angular frequencies that correspond fairly well to the respective onsets of the plateau-like elastic regimes. From this experimental fact, we deduced that the low angular frequency anomaly could be linked to the relaxation of the Brownian stress emerging when filler

Table 2 Low- and high-frequency viscosities (η'_0, η'_{inf}), Pecelet relaxation times τ_p , and angular frequencies ω_p as a function of filler content x at the reference temperature $T_0 = 273$ K. τ_p is calculated according to Eq. 7 with an average radius $\bar{a} = 12.5$ nm of the nanoparticles

x %	η'_0 (Pa.s)	η'_{inf} (Pa.s)	τ_p (s)	ω_p (1/s)
0 (DGEBA pure)	–	10,275	–	–
5	–	10,578	17.2	0.058
10	–	12,767	20.7	0.048
20	37,426	21,347	34.8	0.029
30	145,374	67,136	109	0.009
40	164,0967	575,439	937	0.001

distributions with the highest entropy are disturbed by shear. At high temperatures (or low frequencies), the Brownian relaxation can unambiguously be observed because strain-induced hydrodynamic stresses do instantaneously relax. Due to the small size of the nanoparticles, the Brownian relaxation can be observed down to a filler concentration as low as 5 wt %. To our best knowledge, the Brownian relaxation was not observed experimentally for dilute suspension ($x < 20$) yet. At intermediate angular frequencies, the α -process of the matrix superimposing the Brownian stress relaxation starts taking more and more influence on the viscoelastic behavior of the nanocomposites. Finally, at high angular frequencies, at least the viscoelastic behavior of the DGEBA- x % SiO₂ systems is dominated by the α -process of the matrix.

Acknowledgments This work was kindly supported by the National Research Fund, Luxembourg.

References

- Alberola ND, Benzarti K, Bas C, Bomal Y (2001) Interface effects in elastomers reinforced by modified precipitated silica. *Polym Compos* 22:312–325. doi:10.1002/pc.10540
- Baller J, Becker N, Ziehmer M, Thomassey M, Zielinski B, Müller U, Sanctuary R (2009) Interactions between silica nanoparticles and an epoxy resin before and during network formation. *Polymer* 50:3211–3219. doi:10.1016/j.polymer.2009.05.020
- Baller J, Thomassey M, Ziehmer M, Sanctuary R (2011) Thermal and chemical glass transition of thermosets in the presence of two types of inorganic nanoparticles. *Thermoplastic and thermosetting polymers and composites*
- Chabert E, Bornert M, Bourgeat-Lami E, Cavaillé JY, Dendievel R, Gauthier C, Putaux JL, Zaoui A (2004) Filler-filler interactions and viscoelastic behavior of polymer nanocomposites. *Mat Sci Eng A* 381:320–330. doi:10.1016/j.msea.2004.04.064
- Corezzi S, Beiner M, Huth H, Schroter K, Capaccioli S, Casalini R, Fioretto D, Donth E (2002) Two crossover regions in the dynamics of glass forming epoxy resins. *J Chem Phys* 117:2435–2448. doi:10.1063/1.1486214
- Dudkin BN, Zainullin GG, Krivoshapkin PV, Krivoshapkina EF, Ryazanov MA (2008) Influence of nanoparticles and nanofibers of aluminum oxide on the properties of epoxy composites. *Glas Phys Chem* 34:187–191. doi:10.1134/S1087659608020120
- Graebling D, Muller R, Palierné JF (1993) Linear viscoelastic behavior of some incompatible polymer blends in the melt. Interpretation of data with a model of emulsion of viscoelastic liquids. *Macromolecules* 26:320–329. doi:10.1021/ma00054a011
- Hanse C (2002). Patent Application WO 02/083776 A1
- Inoubli R, Dagréou S, Lapp A, Billon L, Peyrelasse J (2006) Nanostructure and mechanical properties of polybutylacrylate filled with grafted silica particles. *Langmuir* 22:6683–6689. doi:10.1021/la0607003
- Jaber E, Luo H, Li W, Gersappe D (2011) Network formation in polymer nanocomposites under shear. *Soft Matter* 7:3852–3860. doi:10.1039/C0SM00990C
- Johnsen BB, Kinloch AJ, Mohammed RD, Taylor AC, Sprenger S (2007) Toughening mechanisms of nanoparticle-modified epoxy polymers. *Polymer* 48:530–541. doi:10.1016/j.polymer.2006.11.038
- Kinloch AJ, Masania K, Taylor AC, Sprenger S, Egan D (2008) The fracture of glass-fibre-reinforced epoxy composites using nanoparticle-modified matrices. *J Mater Sci* 43:1151–1154. doi:10.1007/s10853-007-2390-3
- Kinloch AJ, Taylor AC (2006) The mechanical properties and fracture behavior of epoxy-inorganic micro- and nano-composites. *J Mater Sci* 41:3271–3297. doi:10.1007/s10853-005-5472-0
- Le Pluart L, Duchet J, Sautereau H, Halley P, Gerard JF (2004) Rheological properties of organoclay suspensions in epoxy network precursors. *Appl Clay Sci* 25:207–219. doi:10.1016/j.clay.2003.11.004
- Lionberger RA, Russel WB (1997) A Smoluchowski theory with simple approximations for hydrodynamic interactions in concentrated dispersions. *J Rheol* 41:399–425. doi:10.1122/1.550873
- Müller U, Philipp M, Thomassey M, Sanctuary R, Krüger JK (2013) Temperature modulated optical refractometry: a quasi-isothermal method to determine the dynamic volume expansion coefficient. *Thermochim Acta* 555:17–22. doi:10.1016/j.tca.2012.12.011
- Ngai KL, Plazek DJ (1995) Identification of different modes of molecular motion in polymers that cause thermorheological complexity. *Rubber Chem Tech* 68:376–434. doi:10.5254/1.3538749
- Palierné JF (1989) Linear rheology of viscoelastic emulsions with interfacial tension. *Rheologica Acta* 29:204–214. doi:10.1007/bf01331356
- Sanctuary R, Baller J, Krüger JK, Schaefer D, Bactavatchalou R, Wetzel B et al. (2006) Complex specific heat capacity of two nanocomposite systems. *Thermochim Acta* 445:111–115. doi:10.1016/j.tca.2005.05.024
- Schröter K, Donth E (2002) Comparison of shear response with other properties at the dynamic glass transition of different glass formers. *J Non-Cryst Solids* 307:270–280. doi:10.1016/S0022-3093(02)01476-X
- Shikata T, Pearson DS (1994) Viscoelastic behavior of concentrated spherical suspensions. *J Rheol* 38(3):601–616. doi:10.1122/1.550477
- Sprenger S, Eger C, Kinloch AJ, Lee JH, Taylor AC, Egan D (2003) Nano-modified ambient temperature curing epoxy adhesives. *Adhäsion Kleben Dichten* 3: 24e8.
- Suzuki N, Ito M, Yatsuyanagi F (2005) Effects of rubber/filler interactions on deformation behavior of silica filled SBR systems. *Polymer* 46:193–201. doi:10.1016/j.polymer.2004.10.066
- Watanabe H, Yao ML, Yamagishi A, Osaki K, Shikata T, Niwa H, Morishima Y (1996) Nonlinear rheological behaviour of a concentrated spherical silica suspension. *Rheol Acta* 35:433–445. doi:10.1007/BF00368994
- Watanabe H, Yao ML, Sato T, Osaki K (1997) Non-Newtonian flow behaviour of diblock copolymer micelles: Shear-thinning in a nonentangling matrix. *Macromolecules* 30:5905–5912. doi:10.1021/ma961867d
- Van der Werff JC, de Kruijff C G, Blom C, Mellema J (1989) Linear viscoelastic behavior of dense hard sphere dispersions. *Phys Rev A* 39(2):795–807. doi:10.1103/PhysRevA.39.795
- Vignaux-Nassiet V, Allal A, Montfort JP (1998) Emulsion Models and rheology of filled polymers. *Eur Polym J* 34(3/4):309–322. doi:10.1016/S0014-3057(97)00142-0
- Wetzel B, Hauptert F, Zhang MQ (2003) Epoxy nanocomposites with high mechanical and tribological performance. *Compos Sci Technol* 63:2055–2067. doi:10.1016/S0266-3538(03)00115-5
- Winter H (2013) Glass transition as rheological inverse of gelation. *Macromolecules* 46:2425–2432. doi:10.1021/ma400086v